New Measurements of the Deuteron to Proton F_2 Structure Function Ratio

D. Biswas,[1] F. Gonzalez,[2] W. Henry,[3] A. Karki,[4] C. Morean,[5] A. Nadeeshani,[1] A. Sun,[6] D. Abrams,[7] Z. Ahmed,[8] B. Aljawrneh,[9] S. Alsalmi,[10] R. Ambrose,[8] W. Armstrong,[11] A. Asaturyan,[12] K. Assumin-Gyimah,[4] C. Ayerbe Gayoso,[13,4] A. Bandari,[13] S. Basnet,[8] V. Berdnikov,[14] H. Bhatt,[4] D. Bhetuwal,[4] W. U. Boeglin,[15] P. Bosted,[13] E. Brash,[16] M. H. S. Bukhari,[17] H. Chen,[7] J. P. Chen,[3] M. Chen,[7] M. E. Christy,[1,3] S. Covrig,[3] K. Craycraft,[5] S. Danagoulian,[9] D. Day,[7] M. Diefenthaler,[3] M. Dlamini,[18] J. Dunne,[4] B. Duran,[11] D. Dutta,[4] R. Ent,[3] R. Evans,[8] H. Fenker,[3] N. Fomin,[5] E. Fuchey,[19] D. Gaskell,[3] T. N. Gautam,[1] F. A. Gonzalez,[2] J. O. Hansen,[3] F. Hauenstein,[20] A. V. Hernandez,[14] T. Horn,[14] G. M. Huber,[8] M. K. Jones,[3] S. Joosten,[21] M. L. Kabir,[4] C. Keppel,[3] A. Khanal,[15] P. M. King,[18] E. Kinney,[22] M. Kohl,[1] N. Lashley-Colthirst,[1] S. Li,[23] W. B. Li,[13] A. H. Liyanage,[1] D. Mack,[3] S. Malace,[3] P. Markowitz,[15] J. Matter,[7] D. Meekins,[3] R. Michaels,[3] A. Mkrtchyan,[12] H. Mkrtchyan,[12] Z. Moore,[24] S.J. Nazeer,[1] S. Nanda,[4] G. Niculescu,[24] I. Niculescu,[24] D. Nguyen,[7] Nuruzzaman,[25] B. Pandey,[1] S. Park,[2] E. Pooser,[3] A. Puckett,[19] M. Rehfuss,[11] J. Reinhold,[15] B. Sawatzky,[3] G. R. Smith,[3] H. Szumila-Vance,[3] A.S. Tadepalli,[25] V. Tadevosyan,[12] R. Trotta,[14] S. A. Wood,[3] C. Yero,[15] and J. Zhang[2]
(for the Hall C Collaboration)

[1] *Hampton University, Hampton, Virginia 23669, USA*
[2] *Stony Brook University, Stony Brook, New York 11794, USA*
[3] *Thomas Jefferson National Accelerator Facility, Newport News, Virginia 23606, USA*
[4] *Mississippi State University, Mississippi State, Mississippi 39762, USA*
[5] *University of Tennessee, Knoxville, Tennessee 37996, USA*
[6] *Carnegie Mellon University, Pittsburgh, Pennsylvania 15213, USA*
[7] *University of Virginia, Charlottesville, Virginia 22903, USA*
[8] *University of Regina, Regina, Saskatchewan S4S 0A2, Canada*
[9] *North Carolina A & T State University, Greensboro, North Carolina 27411, USA*
[10] *Kent State University, Kent, Ohio 44240, USA*
[11] *Temple University, Philadelphia, Pennsylvania 19122, USA*
[12] *A.I. Alikhanyan National Science Laboratory (Yerevan Physics Institute), Yerevan 0036, Armenia*
[13] *The College of William & Mary, Williamsburg, Virginia 23185, USA*
[14] *Catholic University of America, Washington, DC 20064, USA*
[15] *Florida International University, University Park, Florida 33199, USA*
[16] *Christopher Newport University, Newport News, Virginia 23606, USA*
[17] *Jazan University, Jazan 45142, Saudi Arabia*
[18] *Ohio University, Athens, Ohio 45701, USA*
[19] *University of Connecticut, Storrs, Connecticut 06269, USA*
[20] *Old Dominion University, Norfolk, Virginia 23529, USA*
[21] *Argonne National Laboratory, Lemont, Illinois 60439, USA*
[22] *University of Colorado Boulder, Boulder, Colorado 80309, USA*
[23] *University of New Hampshire, Durham, New Hampshire 03824, USA*
[24] *James Madison University, Harrisonburg, Virginia 22807, USA*
[25] *Rutgers University, New Brunswick, New Jersey 08854, USA*

(Dated: May 28, 2024)

Nucleon structure functions, as measured in lepton-nucleon scattering, have historically provided a critical observable in the study of partonic dynamics within the nucleon. However, at very large parton momenta it is both experimentally and theoretically challenging to extract parton distributions due to the probable onset of non-perturbative contributions and the unavailability of high precision data at critical kinematics. Extraction of the neutron structure and the d-quark distribution have been further challenging due to the necessity of applying nuclear corrections when utilizing scattering data from a deuteron target to extract free neutron structure. However, a program of experiments has been carried out recently at the energy-upgraded Jefferson Lab electron accelerator aimed at significantly reducing the nuclear correction uncertainties on the d-quark distribution function at large partonic momentum. This, then, allows leveraging the vast body of deuterium data covering a large kinematic range to be utilized for d-quark PDF extraction. In this paper we present new data from experiment E12-10-002 carried out in Jefferson Lab Experimental Hall C on the deuteron to proton cross–section ratio at large Bjorken-x. These results significantly improve the precision of existing data, and provide a first look at the expected impact on quark distributions extracted from global parton distribution function fits.

Measurements of the nucleon F_2 structure function in inelastic lepton-nucleon scattering and the kinematic evo-

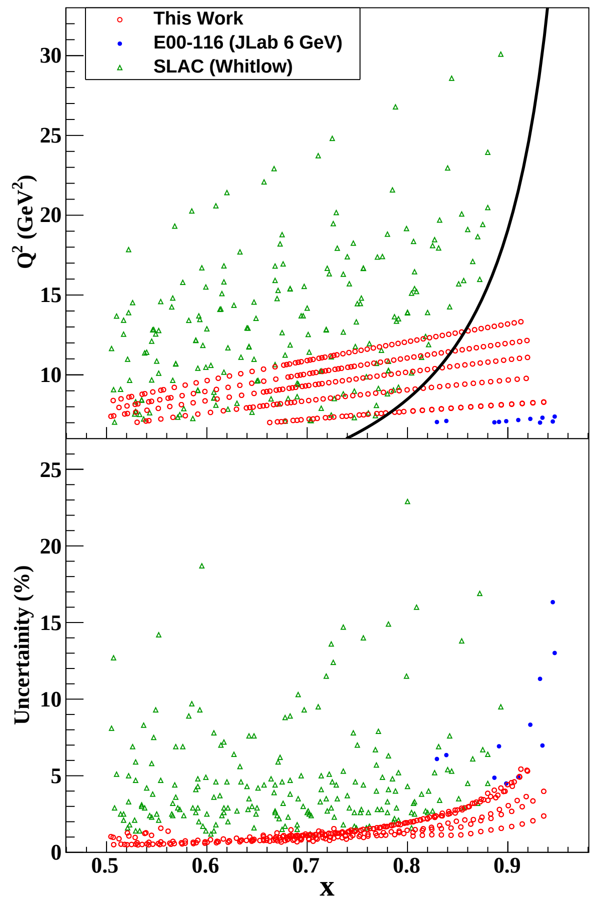

FIG. 1. The top panel shows the kinematic coverage of this work (red circles), compared with the Whitlow reanalysis [10] existing SLAC data (green triangles). The solid blue circles are from JLab's 6 GeV experiment, E00-116. The solid curve indicates $W^2 = 3$ GeV^2, where W is the invariant mass of the produced hadronic system. The statistical uncertainty of the deuteron to hydrogen cross–section ratio from these experiments are shown in the bottom panel.

lution of F_2 occupy a prominent place in the historical development and testing of the theory of the strong interaction, Quantum Chromodynamics (QCD) [1–3]. Such measurements have provided critical data in perturbative QCD (pQCD) fits used to extract quark and gluon distributions and in testing the universality of the pQCD evolution equations of these parton distribution functions (PDFs) [4–6]. While tremendous progress has been made in this endeavor over the last few decades, much is still left to be fully explored. One such example is the longitudinal momentum distribution of the down quarks at large Bjorken-x ($x \to 1$), where the nucleon's momentum is predominantly carried by a single valence quark. While there exists a number of effective theory predictions [5–9] for the ratio of the down to up quark distributions (d/u) at large x, additional experimental data are required to adequately test these. The last few years have seen the completion of three complementary experiments performed at Jefferson Lab utilizing the energy-upgraded CEBAF accelerator and aimed at extracting the neutron to proton F_2 ratio and providing access to d/u at large x. The first of these was the MARATHON [11] experiment in Hall A, which measured ratios of the inclusive structure function F_2 from the A=3 mirror nuclei ^{3}He and ^{3}H, as well as from the deuteron and proton. The second experiment was the BONuS12 [12] experiment in Hall B, which is a follow-up to the BONuS [13–15] experiment, but leveraging the doubling of the beam energy to 12 GeV to access larger x without entering the region of the nucleon resonances. Jefferson Lab (JLab) experiment E12-10-002 (this work) measured $H(e, e')$ and $D(e, e')$ inclusive cross–sections with the aim of extracting the hydrogen and deuterium F_2 structure functions at large x and intermediate Q^2. The new high-precision data from this work, especially when coupled with new nuclear correction data from BONuS12 and MARATHON, will provide new insight into the up and down quark distributions within the nucleon.

The dataset was acquired in February–March of 2018 in Hall C. The experiment used the standard Hall C equipment: the High Momentum Spectrometer (HMS), the SuperHMS (SHMS), and liquid cryogenic hydrogen and deuterium targets. The beam energy was 10.602 GeV and the beam current varied between 30 and 65 μA. The experiment served as one of the commissioning experiments for the new or upgraded Hall C equipment associated with the JLab 12 GeV energy upgrade. The data were acquired in "scans" at a fixed spectrometer angle by varying the central momentum setting and alternating between the 10 cm long hydrogen and deuterium targets. The results presented here stem from five different SHMS scans at (nominal) scattering angles of 21, 25, 29, 33, and 39 degrees. The central momentum varied between 1.3 and 5.1 GeV/c. Additional scans were taken with the HMS at 21 and 59 degrees. The 21 degree data were used as a cross-check between the well understood HMS and the newly constructed SHMS. The 59 degree data are still being analyzed and will not be presented here. The kinematic coverage of this work is shown in Fig.1 in four-momentum transfer Q^2 and x coordinates. Also displayed in Fig.1 are the world data from SLAC (green triangles) and 6 GeV JLab (blue solid circles). The $W^2 < 3$ GeV^2 region, (i.e. to the right of the solid curve), is poorly populated above a Q^2 of about 6 GeV^2. The statistical uncertainties of this work, shown in the top panel of Fig.1, are a vast improvement over existing data.

The SHMS is a new spectrometer installed in Hall C to take advantage of the energy upgrade of the CEBAF accelerator to 12 GeV. [16–18]. Its magnetic layout consists of a horizontal bender, three quadrupoles, and a dipole ($HQ\bar{Q}QD$). The maximum momentum is 11.0 GeV/c, the typical momentum acceptance is -10% to 22% about the central momentum, and the solid angle $\approx$ 4.0 msr. The standard detector package includes a gas Cherenkov

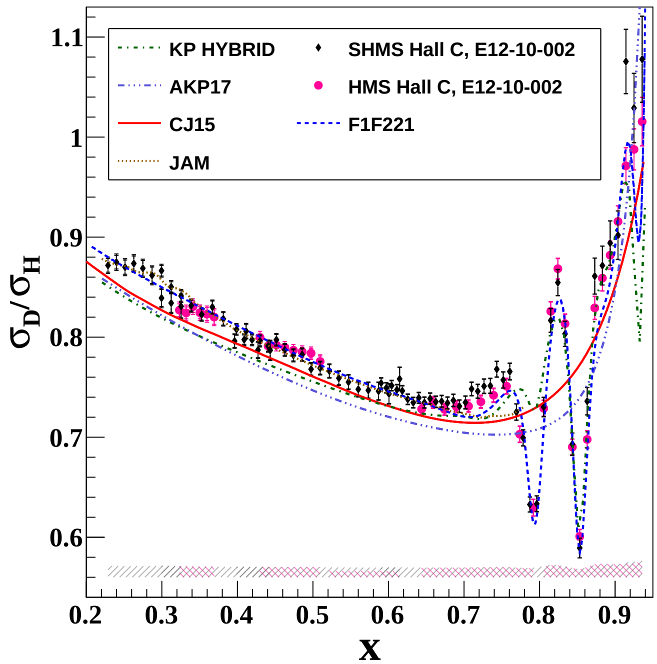

FIG. 2. The σ_D/σ_H ratio as a function of x for a spectrometer angle of 21 deg (Q^2 range from 3.39 to 8.25 GeV^2). The error bars include uncorrelated systematic and statistical errors. The error bands include correlated systematic errors and an overall normalization of 1.1%(see Table I.). F1F221 (blue dashed line) is the model used in this analysis, the other curves are from different PDF fits (see text). Good agreement is observed between the well-understood HMS and newly constructed SHMS spectrometers.

detector (filled with 1 atm of CO_2) and an electromagnetic calorimeter for particle identification (PID), two wire drift chambers for tracking and event reconstruction, and four hodoscope planes used in the event trigger. An additional heavy gas Cherenkov and aerogel detector were present in the detector package but not used in this analysis as they are primarily used for hadron identification.

In the one-photon exchange approximation the differential cross–section for inclusive electron scattering can be written as:

$$\frac{d^2\sigma}{d\Omega dE'} = \sigma_{Mott}\frac{2MxF_2}{Q^2\varepsilon}\left(\frac{1+\varepsilon R}{1+R}\right) \quad (1)$$

Where σ_{Mott} is the Mott cross–section, M is the nucleon mass, Q^2 is the negative of the four-momentum transfer squared, R is the ratio of the longitudinal and transverse reduced cross–sections ($R = \sigma_L/\sigma_T$), ε is the virtual photon polarization, F_2 is the structure function and x is the Bjorken scaling variable. The aim of this work is to obtain the F_2^D/F_2^H ratio, as it presents several advantages theoretically as well as experimentally. By reporting a quantity involving deuterium rather than the ("free") neutron we avoid choosing a particular prescription for treating nuclear effects, allowing theory groups active in this field to extract F_2^n using their own nuclear corrections. Furthermore, the σ_L/σ_T ratio is largely the same for hydrogen and deuterium [19], thus, to first order, the F_2^D/F_2^H ratio is the same as the cross–section ratio.

Experimentally, the cross–section is obtained using the Monte Carlo ratio method [20]

$$\left(\frac{d^2\sigma}{d\Omega\, dE'}\right)_{exp} = \frac{Y_{Data}}{Y_{MC}}\left(\frac{d^2\sigma}{d\Omega\, dE'}\right)_{model} \quad (2)$$

where Y_{Data} is the efficiency and background corrected charge normalized electron yield, Y_{MC} is the Monte Carlo yield obtained using a model cross–section that is radiated using the Mo and Tsai formalism [21, 22], and $\left(\frac{d^2\sigma}{d\Omega\, dE'}\right)_{model}$ is the same model cross–section evaluated at the Born level. The yields were binned in W^2 and then converted to x. Electrons were selected by applying cuts to the noble gas Cherenkov and the energy deposited in the calorimeter normalized by the momentum of the track.

Corrections to Y_{Data} include pion contamination, deadtime, target density, tracking efficiency, trigger efficiency, and backgrounds from the target cell walls. Pions that pass the electron PID cuts were removed using a parameterization of the pion contamination as a function of the scattered electron energy, E'. The computer deadtime was found by comparing the number of triggers found in scalers to the number recorded in the datastream. The electronic deadtime from events being lost at the trigger logic level was measured by injecting a pulser of known frequency at the beginning of the trigger logic chain. These pulser events can be identified using TDC information and compared with the number of events recorded in the scalers. Tracking efficiency was calculated by taking the ratio of events where a track was found to the number of events that passed PID, fiducial and timing cuts. The trigger for this experiment required a signal in 3 of the 4 hodoscope layers and a signal in either the gas Cherenkov or calorimeter. The trigger efficiency was $> 99\%$ and determined by calculating the efficiency of the individual hodoscope planes. Backgrounds from the aluminum cell walls were subtracted from the cryogenic targets by utilizing "dummy" data taken on two aluminum targets placed at the same location as the cryogenic entrance and exit windows. A target density correction was applied to account for a local change in density due to heating from the electron beam. A series of dedicated measurements at various currents up to 80 uA were performed and the charge normalized yields were plotted vs beam current. The density reduction for the hydrogen (deuterium) target was $2.55 \pm 0.74 \frac{\%}{100\ uA}$ ($3.09 \pm 0.84\ \frac{\%}{100\ uA}$). For further details of the analysis see [23–28].

Electrons produced by charge symmetric backgrounds, mainly from neutral pion production (e.g. $\pi^0 \rightarrow \gamma\gamma^* \rightarrow \gamma e^+e^-$), in which the photon decays into a positron and

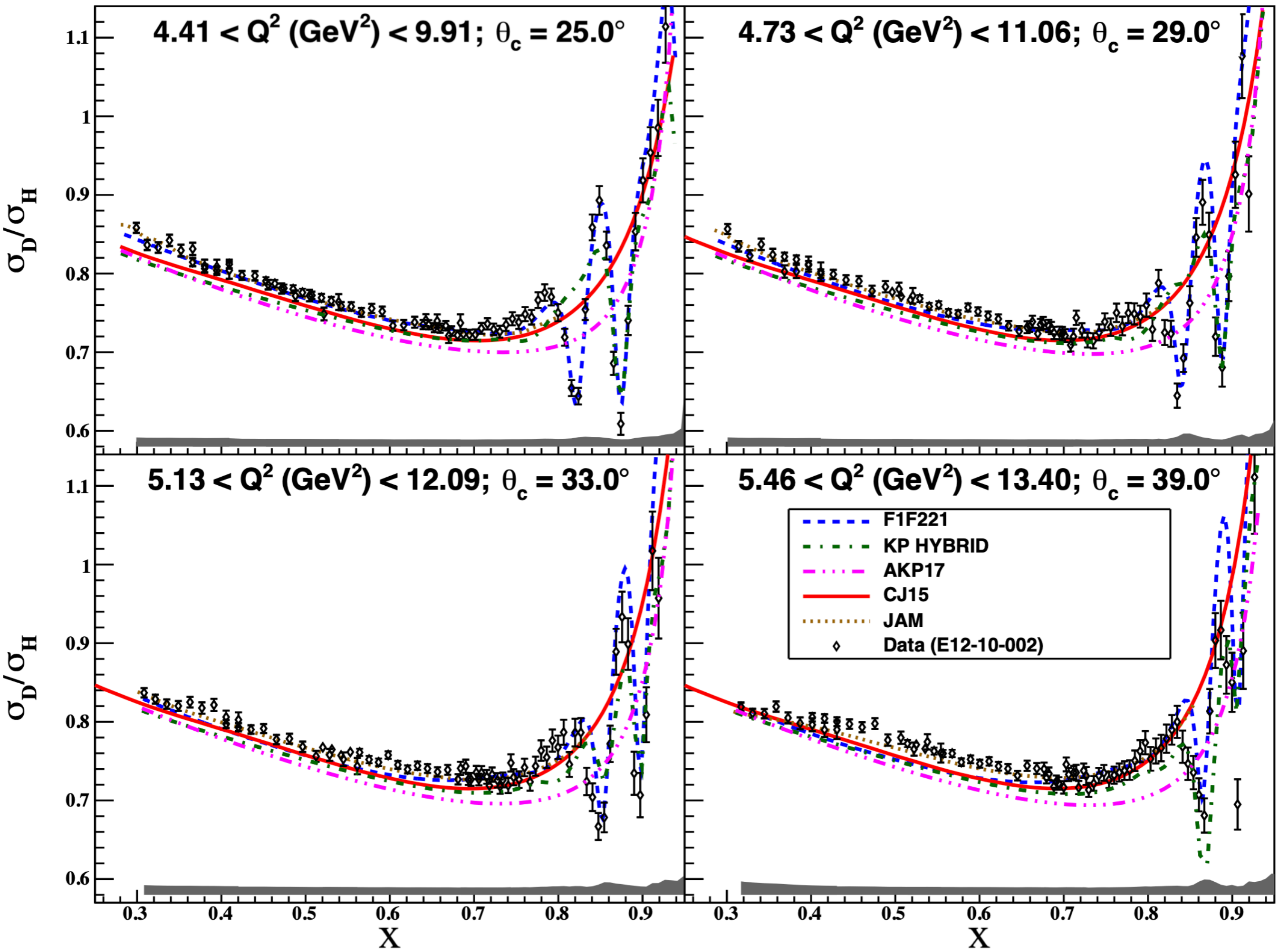

FIG. 3. The σ_D/σ_H ratio as a function of x for SHMS spectrometer angles of 25, 29, 33, and 39 deg. The Q^2 range of each setting is indicated in each panel.

an electron were included in the Monte Carlo yield. This background was measured by reversing the spectrometers' magnet polarity to measure the positron yield. The background was parameterized with a two parameter fit as a function of E'. Due to beam time constraints, positron data was acquired for only three of the five angular settings. To circumvent this limitation, the positron yield was parameterized as described in [29]. The parameterization was then used to extrapolate the positron yield to the kinematic settings where measurements were not available.

The errors in the deuterium to hydrogen cross–section ratio σ_D/σ_H, shown in Table I, are divided into two categories, uncorrelated point-to-point and correlated. An overall normalization uncertainty of 1.1% due to uncertainty in the target density is included in the correlated error. The target density error includes uncertainties from the target temperature and pressure, measured length, thermal contraction, the equation of state used to calculate the density, and the target boiling correc-

Error	Pt. to Pt (%)	Correlated (%)
Statistical	$0.6-5.6(2.9)$	
Charge	$0.1-0.6$	
Target Density	$0.0-0.2$	1.1
Livetime		$0.0-1.0$
Model Dependence		$0.0-2.6(1.2)$
Charge Sym. Background		$0.0-1.4$
Acceptance		$0.0-0.6(0.3)$
Kinematic		$0.0-0.4$
Radiative Corrections		$0.5-0.7(0.6)$
Pion Contamination		$0.1-0.3$
Cherenkov Efficiency		0.1
Total	$0.6-5.7(2.9)$	$1.3-2.9(2.1)$

TABLE I. The error budget for the cross–section ratio σ_D/σ_H. The error after a cut of $W^2 > 3$ GeV^2 is shown in parenthesis, which is a typical cut applied to eliminate the resonance region while performing PDF fits.

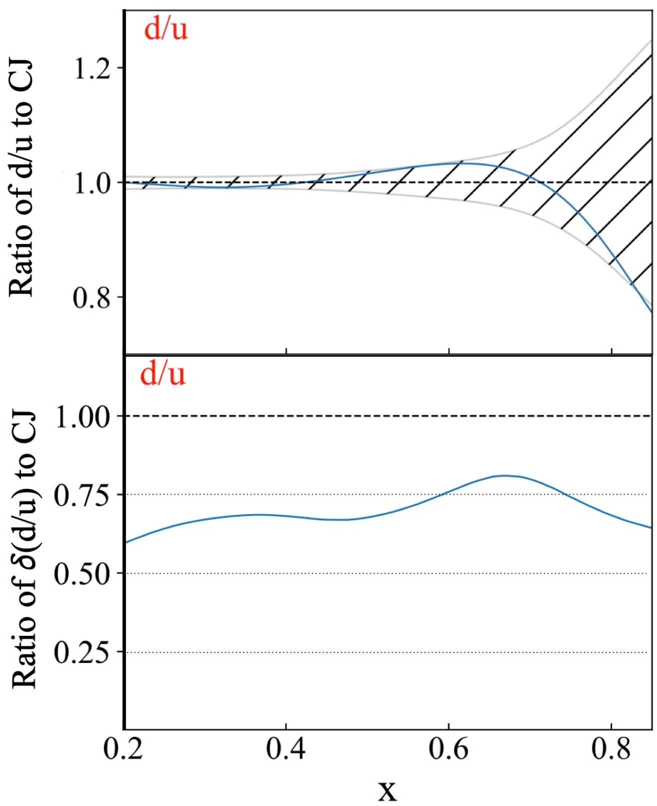

FIG. 4. Top: The blue line shows the relative change in the CJ15 central value of the d/u PDF after data from this analysis are included in the fit. The band represents the error of the fit before the inclusion of this data. Here the lack of data on deuterium at high-x is reflected in the large error. Bottom: The relative error on the CJ15 PDF fit after including data from this experiment. The inclusion of this new data results in a 20-40% reduction of the uncertainty in the d/u PDFs. A cut of $W^2 > 3$ GeV^2 is applied to the data that enters the fit.

tion. Additional point-to-point errors for target density are included to account for runs where the boiling correction was far from the average due to higher or lower beam currents. A Monte Carlo cross–section model dependence error was determined by repeating the analysis using different models and comparing the final σ_D/σ_H result; the largest effects were at higher x values where the resonance region causes the cross–section to change rapidly. Errors from the radiative corrections include a contribution from both the model and the method. The model dependence was determined by scaling the various quasi-elastic contributions to the model. The error associated with the method (0.5%) was taken from [30].

The results of this analysis are summarized in Fig. 2 and Fig. 3. The σ_D/σ_H ratio is shown as a function of x for each of the SHMS spectrometer angles. The curves shown are predictions obtained using four available models: CJ15 [9] (solid red line), AKP17 [7] (dot-dot-dot-dashed violet line), KP Hybrid[8] (dot-dashed line) and JAM [31, 32] (dotted brown line). The model used to extract the cross–section is F1F221 (dashed blue line) which is a improved fit to world data [33] . None of the models shown includes the data from this analysis.

It should be noted that, on average, the results from this work and MARATHON differ by as much as 4.3%. The overall normalization uncertainty for the MARATHON result is 0.55% [34]. For this work the total correlated error is 1.6% in the x range where the data sets overlap. In a recent study[35] where the MARATHON data was included in a global QCD analysis, the data needed to be normalized by +1.9% to agree with existing data. In a CJ15 study [36] it was found the data from this work needed to be shifted down 2.1% to agree with the CJ model [9]. This experiment ran in parallel with E12-10-007 (a measurement of the EMC effect) which observed a 2.0% normalization difference with previous EMC measurements [37]. The direction of this normalization difference is consistent with that found in the CJ15 study. All the aforementioned data agree with the previously available SLAC data, which have large uncertainties [10].

In a recent study by the CJ collaboration, which deploys state-of-the-art deuteron nuclear corrections and leverages recent results, the data from this work was included into their PDF fits. The impact of this work can been seen in Fig. 4. Not only did the inclusion of this data shift the d/u central value at large-x by as much as 20%, but it also reduced the relative error by 20%–40% across the entire x range. Furthermore, this data provides additional constraints on the parameters used in higher twist corrections, the individual d and u quark distributions, and the target mass corrections used in these fits.

In summary, high-precision inclusive measurements on hydrogen and deuterium were performed for Q^2 from 3.4 to 13.4 GeV^2 and x from 0.3 to 0.93. This data, especially when combined with the MARATHON and BoNUS results, has a significant impact on PDF fitting efforts. It can be used, moreover, for quark-hadron duality studies, spin-flavor symmetry breaking, and constraints on nuclear corrections. Additionally, knowledge of PDF fits at large-x is essential for determining high energy cross–sections at the future EIC, where structure function information at large x feeds down through perturbative Q^2 evolution to lower x and higher values of Q^2, and for higher precision neutrino oscillation Monte Carlos for DUNE [38].

This material is based upon work supported by the U.S. Department of Energy, Office of Science, Office of Nuclear Physics under contracts DE-AC05-06OR23177, DE-AC02-05CH11231, DE-SC0013615, and DE-FE02-96ER40950, and by the National Science Foundation (NSF) Grant No. 1913257.

[1] R. E. Taylor, Rev. Mod. Phys. **63**, 573 (1991).
[2] H. W. Kendall, Rev. Mod. Phys. **63**, 597 (1991).
[3] J. I. Friedman, Rev. Mod. Phys. **63**, 615 (1991).
[4] A. Accardi *et al.*, Phys. Rev. D **81**, 034016 (2010).
[5] S. I. Alekhin, Phys. Rev. D **63**, 094022 (2001).
[6] S. I. Alekhin, Phys. Rev. D **68**, 014002 (2003).
[7] S. I. Alekhin, S. A. Kulagin, and R. Petti, Phys. Rev. D **96**, 054005 (2017), arXiv:1704.00204 [nucl-th].
[8] S. A. Kulagin, Phys. Part. Nucl. **50**, 506 (2019), arXiv:1812.11738 [nucl-th].
[9] A. Accardi, L. T. Brady, W. Melnitchouk, J. F. Owens, and N. Sato, Phys. Rev. D **93**, 114017 (2016).
[10] L. W. Whitlow, *Deep Inelastic Structure Functions From Electron Scattering on Hydrogen, Deuterium, and Iron at 0.6-*$GeV^2 \leq Q^2 \leq 30$-GeV^2, Other thesis (1990).
[11] D. Abrams *et al.* (Jefferson Lab Hall A Tritium Collaboration), Phys. Rev. Lett. **128**, 132003 (2022).
[12] M. Amarian, C. Collaboration, *et al.*, CLAS-PROPOSAL PR12-06-113 (2006).
[13] N. Baillie *et al.* (CLAS), Phys. Rev. Lett. **108**, 142001 (2012), [Erratum: Phys.Rev.Lett. 108, 199902 (2012)], arXiv:1110.2770 [nucl-ex].
[14] K. A. Griffioen *et al.*, Phys. Rev. C **92**, 015211 (2015).
[15] S. Tkachenko *et al.* (CLAS Collaboration), Phys. Rev. C **89**, 045206 (2014).
[16] The SHMS 11 GeV/c Spectrometer in Hall C at Jefferson Lab (to be published).
[17] D. Bhetuwal, J. Matter, H. Szumila-Vance, C. Ayerbe Gayoso, M. Kabir, D. Dutta, R. Ent, D. Abrams, Z. Ahmed, B. Aljawrneh, *et al.*, Physical Review C **108** (2023).
[18] D. Bhetuwal *et al.* (The Jefferson Lab Hall C Collaboration), Phys. Rev. Lett. **126**, 082301 (2021).
[19] L. H. Tao *et al.* (E140X), Z. Phys. C **70**, 387 (1996).
[20] M. Murphy *et al.* (The Jefferson Lab Hall A Collaboration), Phys. Rev. C **100**, 054606 (2019).
[21] Y.-S. Tsai, SLAC Preprint SLAC-PUB-848 (1971).
[22] L. W. MO and Y. S. TSAI, Rev. Mod. Phys. **41**, 205 (1969).
[23] F. Araiza Gonzalez, Ph.D. thesis, Stony Brook University (2020).
[24] S. Nadeeshani, Ph.D. thesis, Hampton University (2021).
[25] A. Sun, Ph.D. thesis, Carnegie Mellon University (2022).
[26] D. Biswas, Ph.D. thesis, Hampton University (2022).
[27] A. Karki, Ph.D. thesis, Mississippi State University (2022).
[28] C. Morean, Ph.D. thesis, University of Tennesse (2023).
[29] V. Mamyan, (2012), arXiv:1202.1457 [nucl-ex].
[30] S. Dasu, Ph.D. thesis, University of Rochester (1988).
[31] N. Sato, C. Andres, J. J. Ethier, and W. Melnitchouk (Jefferson Lab Angular Momentum (JAM) Collaboration), Phys. Rev. D **101**, 074020 (2020).
[32] E. Moffat, W. Melnitchouk, T. C. Rogers, and N. Sato (Jefferson Lab Angular Momentum (JAM) Collaboration), Phys. Rev. D **104**, 016015 (2021).
[33] P. E. Bosted and M. E. Christy, Phys. Rev. C **77**, 065206 (2008).
[34] D. e. a. Abrams (Jefferson Lab Hall A Tritium Collaboration), Phys. Rev. Lett. **128**, 132003 (2022).
[35] C. Cocuzza, C. E. Keppel, H. Liu, W. Melnitchouk, A. Metz, N. Sato, and A. W. Thomas (Jefferson Lab Angular Momentum (JAM) Collaboration), Phys. Rev. Lett. **127**, 242001 (2021).
[36] S. Li, private communication (2022).
[37] A. Karki *et al.* (Hall C), Phys. Rev. C **108**, 035201 (2023), arXiv:2207.03850 [nucl-ex].
[38] R. Acciarri *et al.* (Dune Collaboration), (2016), arXiv:1512.06148.